NEW APPROACH TO HIGH-VOLTAGE POWER CAPACITOR FAILURE DETECTION

Meng-Hui Wang*, Zi-Yi Zhan and Meng-Ju Hsieh

Department of Electrical Engineering
National Chin-Yi University of Technology
No. 57, Sec. 2, Chung-Shan Road, Taiping Dist., Taichung City 41101, Taiwan
*Corresponding author: wangmh@ncut.edu.tw

ABSTRACT. *A new approach to detect the failure of high-voltage power capacitor (HVPC) was proposed to allow the prediction of possible failures and categories of a power capacitor. First, a circuit model simulating an HVPC was built for measurement. To determine the characteristics of failure, the chaos synchronization detection was employed to establish the chaos error distribution diagram of voltage and current with the center of gravity of the error distribution (or the chaos eyes) as the features of the failure diagnosis. The advantage of using this approach is that the amount of data from feature capturing is greatly reduced while it is capable of effectively detecting minute changes in the damage state of power capacitor, which allows change of operating state of power capacitor in advance and initiation of response measure before anything serious occurs. Finally, a 22.8kV/100kVAR power capacitor was put to test and it was proven that the new approach had the potential to be used as a tool for online real-time monitoring of power systems.*
Keywords: Chaos synchronization detection, High-voltage power capacitor, Failure detection

1. **Introduction.** A country's economic development and the quality of its people's life depend heavily on the safety, efficiency and steady operations of power systems. In response to the tides of the time, online real-time monitoring of power capacitors is the key to future development. There have been a number of power capacitor test methods proposed in various literature, such as dielectric loss factor ($\tan \delta$) measurement [1], leak current measurement [2], partial discharge [3] and gases dissolved in insulating oil [4]. The leak current refers to the electric current flowing through the surface of a piece of equipment as it is subject to operation voltage. For partial discharge, the electric field concentrates at certain parts inside of a power capacitor, but the insulation defects (e.g., voids or impurities) often lead to partial discharge due to the effects of the electric field strength, resulting in deteriorated insulation performance. The gases dissolved in insulating oil are gases generated in the power capacitor due to internal partial discharge, heat generation or aging of oiled paper. The quantity and type of gases vary depending on type of failures. A new method is proposed to detect the failure features of the high voltage power capacitor in this paper. The voltage and current testing was performed by measuring the line voltage and current of the system to be tested and the chaos synchronization detection (CSD) [5] was introduced to capture failure features. This method required minimal sensors, and thus improved the performance and accuracy of HVPC failure detection. The new approach had the potential to be used as a tool for online monitoring system in the smart grid.

2. The Proposed New Failure Detection Method.

2.1. **Structure of power capacitor.** HVPCs are widely used in power systems as shown in Figure 1. They work by providing adjustment of power factor, control of reactive power and suppression of harmonic waves. The installation of power capacitor achieves reduced loss of power transmission, increased power supply capacity, improved power efficiency and increased system stability. A good power capacitor, therefore, is vital to system stability and normal power supply [6].
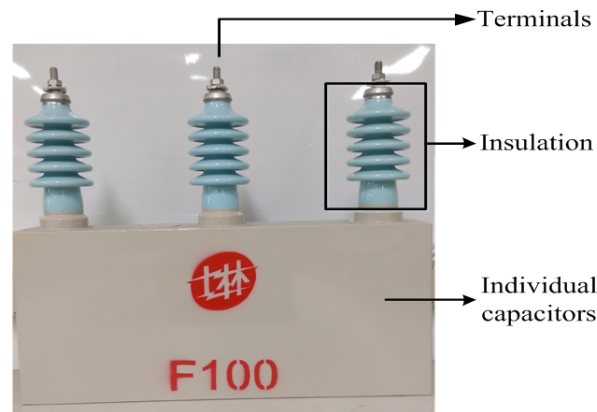

FIGURE 1. Typical 22.8kV/100kVA power capacitor

A power capacitor consists of many single capacitors and its design is made up with combinations of dielectric structures, such as immersed paper or membrane. The electric performance of dielectric combinations is subject to the composition of dielectric material, operating temperature and electric field strength.

2.2. **New failure detection method.** A commercially available HVPC was used for the simulation of its failures. The currents were measured at each phase and voltages between phases as the failure features, as shown in Figure 2, where R_P represents discharge resistor, R_g represents ground resistor, and C represents capacitance value of HVPC. The voltage was measured by dropping the voltage down to within ± 5V with a potential transformer (PT), while the line current was measured by the current transformer (CT).

Figure 3 shows the block diagram of testing system for this study. A 220V AC voltage passed through an induction voltage regulator (IVR) and a transformer for two stages of
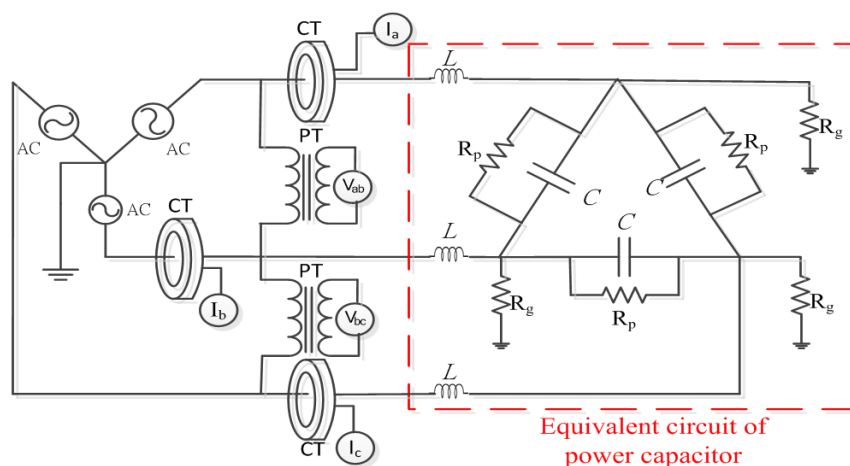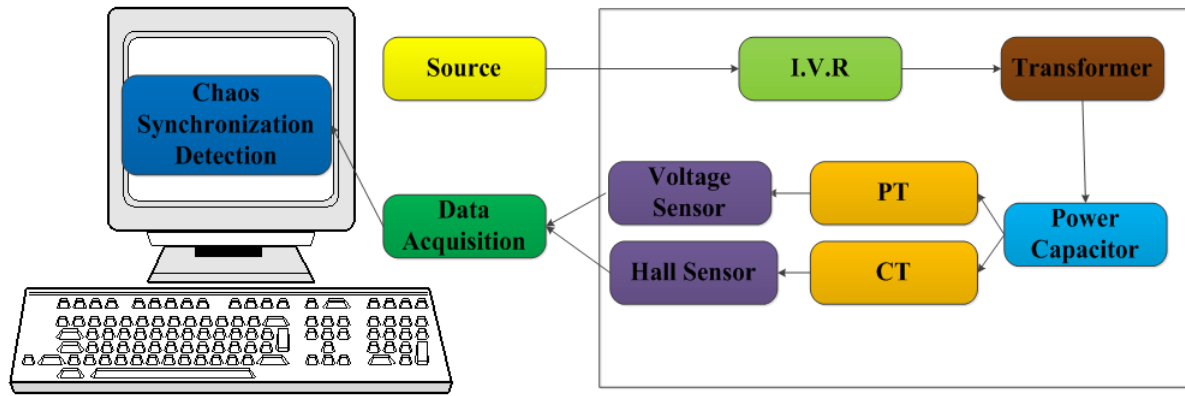

FIGURE 2. Simulation system scheme

FIGURE 3. High-voltage power capacitor failure detection scheme

voltage boosting to 22.8KV. This system measured mainly line current and line to line voltage. The voltage was measured by dropping the voltage down to within ± 5V with a potential transformer (PT), while the line current was measured by converting the current signal to a voltage signal using a Hall sensor as the current passed through a current transformer (CT). The voltage and current measured were transmitted simultaneously to data acquisition (DAQ) for data collection and then to a computer. The voltage and current signals were taken for the CSD with the voltage signal as the master system control signal and current signal as the slave. The CSD results were used to produce chaos error distribution diagram. The chaos eyes of the distribution diagram were extracted as the failure features. The distribution diagram and the changes of the chaos eyes were further analyzed for a clear picture of failures.

Proposed by Edward Norton Lorenz, the chaos synchronization detection method [5] is based on theories that investigate the volatile nature of a nonlinear dynamic system. In a chaotic system, a variation in the initial conditions, however minute it can be, may ultimately lead to huge difference as a result of magnification over a long period of time. In general, a pair of chaotic systems consists of a master system and a slave system. When the master and slave have different initial values, their trajectories will be different as they go on. Researchers have added a controller at the rear end of slave system to track the master in order to bring both of their trajectories into the same track with this controller. This tracking system is called the chaos synchronization. Equation (1) is the equation of chaos synchronization.

$$\lim_{t \to 0} \|Y_{slave}(t) - X_{master}(t)\| = 0 \quad i = 1, 2, \cdots, n \tag{1}$$

where Y_{slave} is slave system data and X_{master} is master system data.

Two Lorenz chaos systems were used for this study. For the purpose of the study, CSD was introduced to generate the chaos error distribution diagram and the chaos eyes of the diagram were chosen as the features for the identification of HVPC failures. Therefore, the control signal of the master system was defined as the phase voltage while that of the slave the line current. Equations (2) and (3) are the master and slave systems, respectively. The dynamic error state equation is expressed in matrix form shown in Equation (4).

$$\begin{cases} \dot{x}_1 = \alpha(x_2 - x_1) \\ \dot{x}_2 = \beta x_1 - x_1 x_3 - x_2 \\ \dot{x}_3 = x_1 x_2 - \gamma x_3 \end{cases} \tag{2}$$

$$\begin{cases} \dot{y}_1 = \alpha(x_2 - x_1) \\ \dot{y}_2 = \beta y_1 - x_1 y_3 - y_2 \\ \dot{y}_3 = y_1 y_2 - \gamma y_3 \end{cases} \tag{3}$$

$$
\begin{bmatrix} \dot{e}_1 \\ \dot{e}_2 \\ \dot{e}_3 \end{bmatrix} = \begin{bmatrix} -\alpha & \alpha & 0 \\ \beta & -1 & 0 \\ 0 & 0 & -\lambda \end{bmatrix} \begin{bmatrix} e_1 \\ e_2 \\ e_3 \end{bmatrix} + \begin{bmatrix} y_2 y_3 - x_2 x_3 \\ -y_1 y_3 + x_1 x_3 \\ y_1 y_2 - x_1 x_2 \end{bmatrix} \tag{4}
$$

where x is the master system data; y is the slave system data; e_1, e_2 and e_3 are the errors between master and slave; and α, β and γ are the parameters for error adjustment; $\alpha = 10$, $\beta = 28$ and $\gamma = (-8/3)$ in this case. The errors e_1 and e_2 were adopted for the chaos error distribution diagram because it made it easier for obvious distinction and to capture the chaos eyes of the distribution diagram [7]. Figure 4 shows a typical chaos error distribution diagram and its chaos eyes. The X and Y values of positive and negative domains calculated were C_1, C_2, C_3 and C_4. The coordinates of their intersections were the chaos eyes, which can be used for the features of the failure detection.
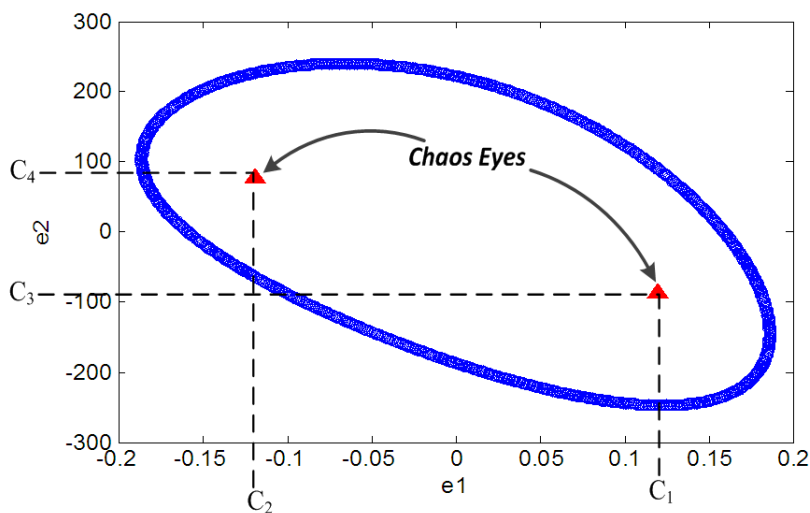

FIGURE 4. Typical chaos error distribution diagram and chaos eyes

TABLE 1. High-voltage power capacitor parameters

Voltage rating, V	22.8KV
Harmonic suppression inductance, L	0.5H
Capacitance, C	0.206uF
Insulation resistance, R_g	3000MΩ
Discharge resistance, R_p	85MΩ

3. **Simulation Results and Discussion.** A 22.8KV/100kVAR HVPC was deployed for the study with the internal element parameters provided in Table 1. The values of these parameters were provided by the manufacturer based on pre-delivery tests. The internal capacitance, inductance and insulation resistance attenuation were simulated for the power capacitor. The simulation consisted of single-phase power capacitance attenuation, simultaneous capacitance attenuation for all 3 phases, harmonic suppression inductance attenuation, and insulation resistance attenuation. The single capacitance attenuated from normal to 40%, the inductance from 0.5H to 0.1H and the insulation resistance from 3000MΩ to 300MΩ.

3.1. **Single-phase power capacitor attenuation.** The single-phase capacitance attenuation test was conducted with a good capacitance attenuating down to 40%. Figure 5 is the chaos error distribution diagram of V_{AB} and I_A with 5% capacitance attenuation at A-phase, and the chaos error distribution diagram of V_{AB} and I_B. Figure 6(a) is the trend
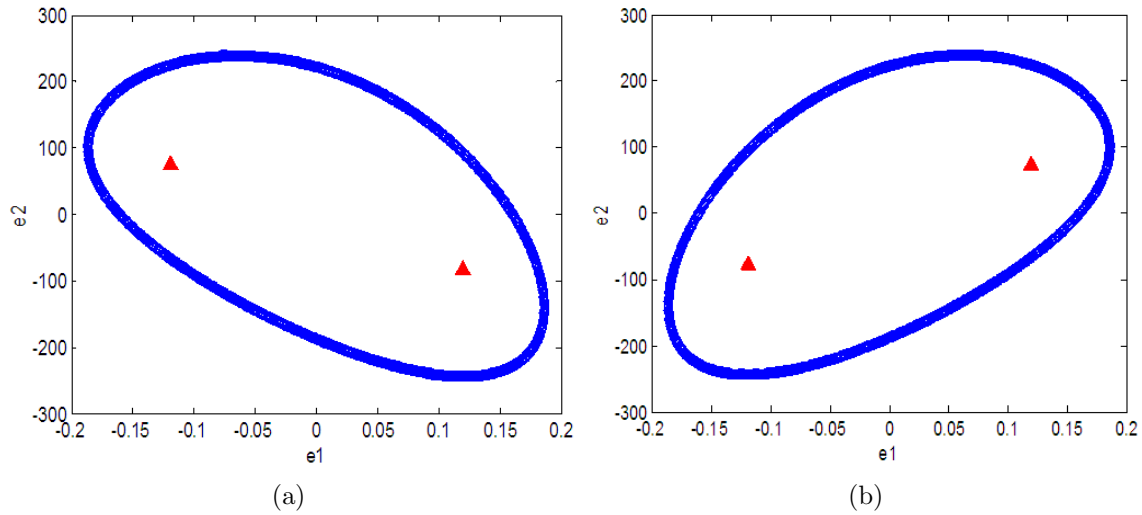
(a)   (b)

FIGURE 5. Chaos error distribution diagram (a) V_{AB} and I_A, (b) V_{AB} and I_B

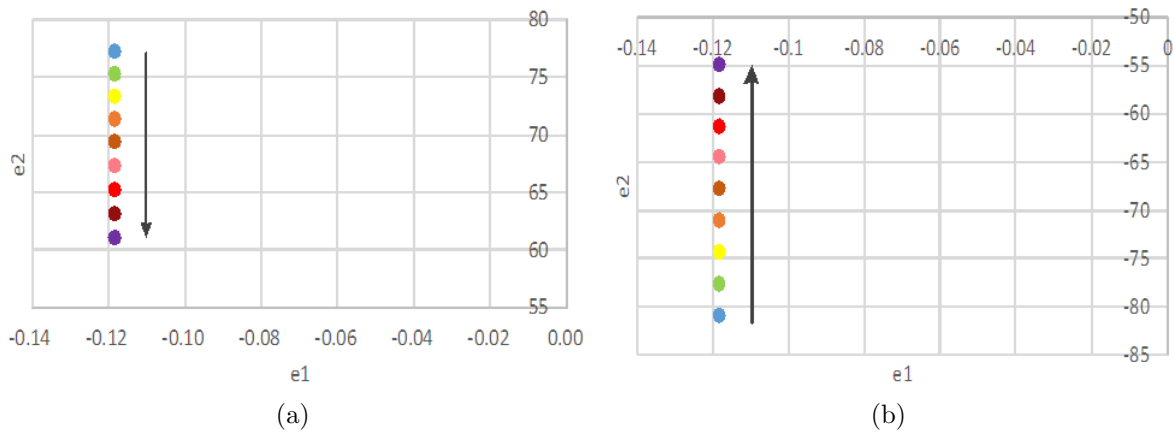(a)   (b)

FIGURE 6. A-Phase capacitance dropping from normal down to 40% (a) trend of left chaos eye of V_{AB} and I_A, (b) trend of right chaos eye of V_{AB} and I_B

of left chaos eye of V_{AB} and I_A with phase A capacitance dropping from normal down to 40%, which indicates that the chaos eye dropped from 78 to 60 along the Y-axis as the A-phase capacitance attenuated. Figure 6(b) is the trend of left chaos eye of V_{AB} and I_B with A-phase capacitance dropping from normal down to 40%, which indicates that the chaos eye rose from -80 to -55 as A-phase capacitance attenuated, exactly opposite as opposed to the attenuation in Figure 6(b). As the A-phase capacitance of single phase attenuated, no significant change was detected in the current of C-phase.

3.2. **Harmonic suppression inductance attenuation.** The harmonic suppression inductance attenuated from 0.5H to 0.1H with 10% of attenuation at every occasion. An approximate direction was identified in the trend, as shown in Figure 7(a). This trend was somewhat incompatible with that of capacitance attenuation with attenuation from -1 down to -3.25 along X-axis and from 80 up to 170 along Y-axis. Figure 7(b) is the right chaos eye trend of A-phase inductance attenuating from normal down to 0.1V_{AB} and I_A. Figure 7 provides a clear trend picture of both chaos eyes using the proposed new method.
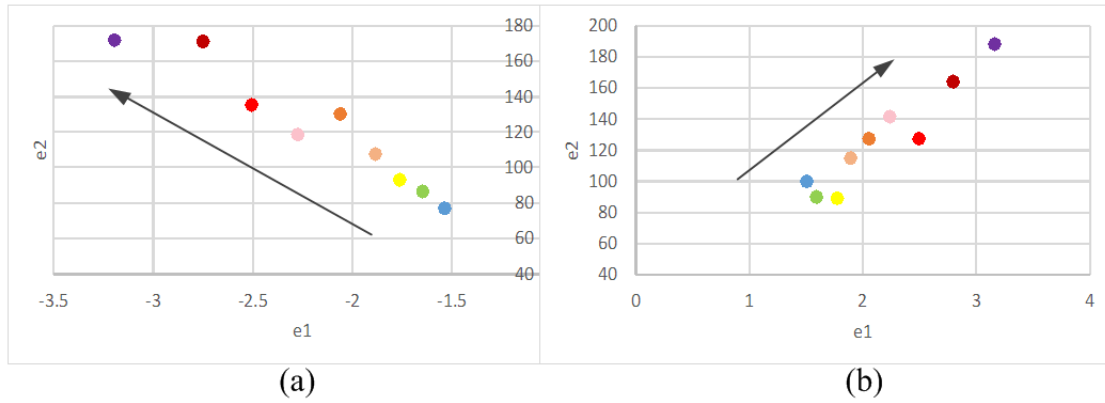
FIGURE 7. A-Phase inductance attenuating from normal to 0.1H (a) trend of left chaos eye of V_{AB} and I_A, (b) trend of right chaos eye of V_{AB} and I_B
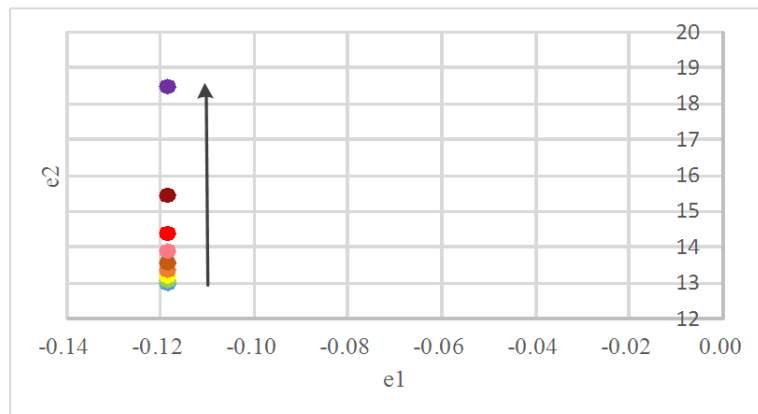

FIGURE 8. Left chaos eye trend of V_{AB} and I_A with A-phase insulation resistance attenuating
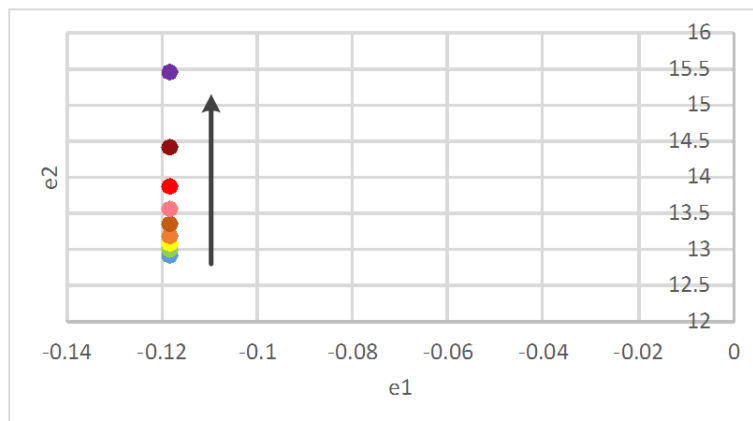

FIGURE 9. Left chaos eye trend of V_{AB} and I_B with B-phase insulation resistance attenuating

3.3. **Insulation resistance attenuation.** For the attenuation of insulation resistance, the attenuation started from 3000MΩ and dropped down to 300MΩ with 10% of attenuation at every occasion. Figure 8 is the chaos eye trend of V_{AB} and I_A of A-phase insulation resistance attenuating from 3000MΩ down to 300MΩ. The chaos eye trend of insulation resistance indicated no change in X-axis but violent changes along Y-axis from 13 at 3000MΩ up to nearly 18.5 at 300MΩ. There was no notable difference with attenuation down to 900MΩ until the attenuation reached 600MΩ or even 300MΩ where there was

a change in proportion in the Y-axis. This demonstrated that the damage of insulation resistance had led to serious destruction of the power capacitor. Figure 9 is the chaos eye trend of V_{AB} and I_B of B-phase insulation resistance attenuating from 3000MΩ down to 300MΩ. The changes were similar to those in Figure 9 except that the increased reached only 15 in Y-axis.

4. **Conclusion.** This paper proposes using line current and line to line voltage as failure detection signals for high voltage power capacitor. The CSD was used to capture the minute changes before the failure. The trends of chaos eye have been adopted as an important basis for power capacitor failure detection. Three conclusions are proposed in this research.

(a) The new method can combine artificial intelligence method, such as extension clustering method for fault diagnosis of power capacitor in the future.

(b) The proposed new approach is easily realizable in the form of integrated circuits, which will be potential in development of real-time fault detection tool in HVPC.

(c) The proposed method can be also used for fault detecting system in other high-voltage power equipments.

REFERENCES

[1] J. Xu and C. P. Wong, Dielectric behavior of ultrahigh-k carbon black composites for embedded capacitor applications, *Proc. of Electronic Components and Technology*, vol.2, pp.1864-1869, 2005.
[2] J. Fan, N. Mi and S. X. D. Tan, Voltage drop reduction for on-chip power delivery considering leakage current variations, *The 25th International Conference of Computer Design*, Lake Tahoe, CA, pp.78-83, 2007.
[3] L. Ghirelli, W. Koltunowicz, A. Pigini, S. Rama Prasath and A. Yellaiah, Acoustical method for partial discharge detection in high power capacitors, *International Conference on Partial Discharge*, Canterbury, pp.92-93, 1993.
[4] C. Feng, J. D. Zhou, F. Yu and G. Honj, Research on power capacitor internal fault criterion, *The 14th International Conference on Intelligent System Design and Engineering Application*, Okinawa, Japan, pp.841-844, 2014.
[5] C. Sparrow, An introduction to the Lorenz equations, *IEEE Trans. Circuits and Systems*, vol.30, no.8, pp.533-542, 1983.
[6] IEEE Standards Association, IEEE recommended practice for testing insulation resistance of electric machinery, *IEEE Power and Energy Society*, pp.1-37, 2014.
[7] M. H. Wang, M. L. Huang and K. J. Liou, Application of extension theory with chaotic signal synchronization to detect islanding effect of photovoltaic power system, *International Journal of Photoenergy*, vol.2015, 2015.